

SEPARATION BETWEEN $d_{5/2}$ AND $s_{1/2}$ NEUTRON
SINGLE PARTICLE STRENGTH IN $^{15}\text{N}^*$ **C.E. MERTIN^a, D.D. CAUSSYN^a, A.M. CRISP^a, N. KEELEY^b
K.W. KEMPER^a, O. MOMOTYUK^a, B.T. ROEDER^a, A. VOLYA^a^aDepartment of Physics, Florida State University
Tallahassee, Florida, 32306-4350, USA^bNational Centre for Nuclear Research
Andrzeja Sołtana 7, 05-400 Otwock, Poland*(Received November 6, 2013)*

The separation between single particle levels in nuclei plays the dominant role in determining the location of the neutron drip line. The separation also provides a test of current crossed shell model interactions if the experimental data is such that multiple shells are involved. The present work uses the $^{14}\text{N}(d,p)^{15}\text{N}$ reaction to extract the $2s_{1/2}$, and $1d_{5/2}$ total neutron single particle strengths and then compares these results with a shell model calculation using a p - sd crossed shell interaction to identify the J^π of all levels in ^{15}N up to 11 MeV in excitation.

DOI:10.5506/APhysPolB.45.159

PACS numbers: 21.60.Cs, 21.10.Jx, 25.45.Hi

1. Introduction

The nucleus ^{15}N was a source of early shell model studies [1] because it has a large number of unnatural parity states that were seen as a puzzle since it has two sd states around 5.3 MeV and then a multiplet of sd states around 7.7 MeV. In addition, around 9 MeV in excitation, negative parity states appear mixed with additional positive parity states. A detailed measurement of the $^{14}\text{N}(d,p)$ reaction at bombarding energies of 7, 8, and 9 MeV when coupled to an earlier work that focused on the ground state strengths in the p shell provided single particle strengths for all states in ^{15}N up to 10 MeV in excitation that displayed enough experimental yield to extract angular distributions [2, 3]. These experimental results were then used by Lie and Engeland [4] to test their weak coupling shell model calculations. Their shell

* Presented at the XXXIII Mazurian Lakes Conference on Physics, Piaski, Poland, September 1–7, 2013.

** This work was supported by the U.S. Department of Energy and the U.S. National Science Foundation.

model calculations were compared to the experimentally observed levels in ^{15}N [5] with the aim of assigning J^π values to the levels whose presence were known but with ambiguous spin parity values. Also, there was the possibility that these calculations could lead to the finding of new levels in this nucleus.

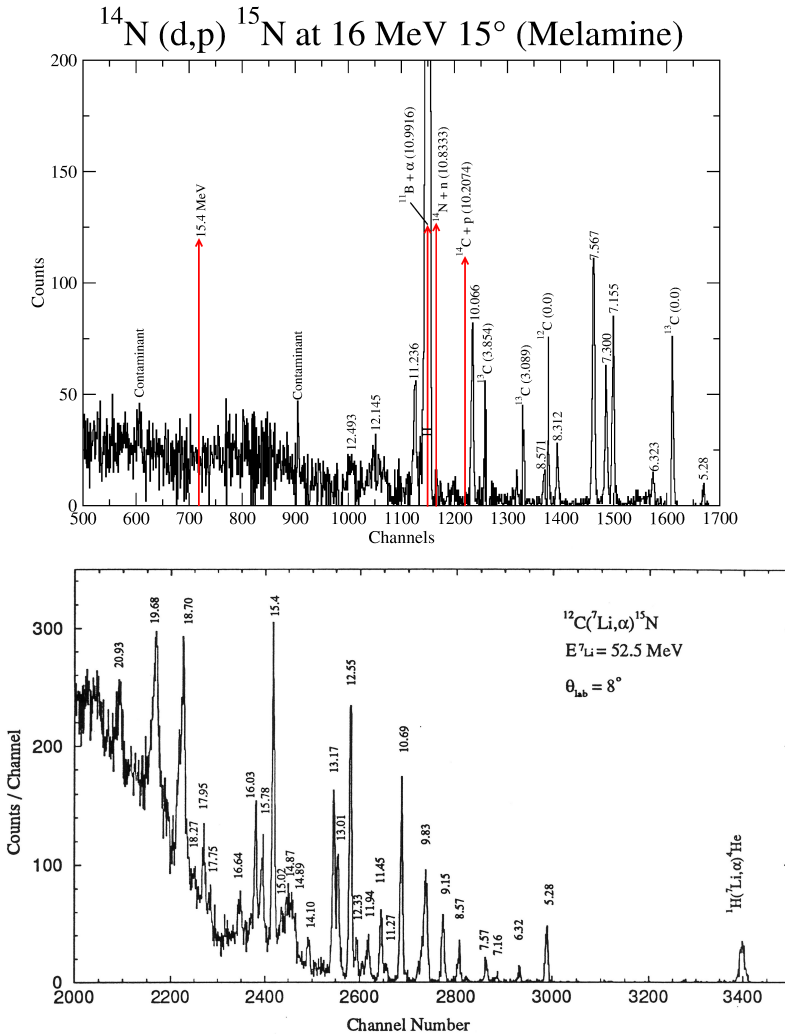


Fig. 1. These spectra show the differences between the single particle transfer reaction $^{14}\text{N}(d,p)$ versus that of the three particle transfer reaction $^{12}\text{C}(^7\text{Li},\alpha)$ [9]. In the three particle transfer, the higher energy states are more strongly populated than those at lower energy states. The inverse is true for the single particle transfer, with the lower energy states being much stronger than the higher energy states.

At about the same time as the calculations of Lie and Engeland were taking place, the use of three particle transfer reactions to locate mirror states in light nuclei was realized [6, 7] including a study to determine the location of mirror states in ^{15}N – ^{15}O [8]. These and other studies [8] discovered a rich spectrum with quite different population strengths from those observed in the (d, p) reaction. While the (d, p) reaction seemed to have little or no strength above 11 MeV, multi-particle transfer reactions populated states up to 20 MeV or more in ^{15}N . The present work uses the higher energy deuteron bombarding energy of 16 MeV to explore this higher energy excitation region with the $^{14}\text{N}(d, p)$ reaction. Figure 1 is a comparison of spectra from the present $^{14}\text{N}(d, p)^{15}\text{N}$ work and that from previously measured spectra for $^{12}\text{C}(^7\text{Li}, \alpha)^{15}\text{N}$ [9]. Note the presence of strong isolated peaks in $(^7\text{Li}, \alpha)$ around 12, 13, and 15 MeV in excitation that are absent in the single neutron transfer spectrum.

In addition to new experimental data, shell model calculations were carried out that used an unrestricted p – sd valence space and an interaction Hamiltonian taken from the work of Utsuno and Chiba [10]. In addition to giving a high quality description of the $0\hbar\omega$ and $1\hbar\omega$ states, this interaction was found to describe well multiparticle correlations in this mass range as well as alpha clustering features [11]. Time dependent and traditional shell model techniques were used for the calculations with the code COSMO [12].

2. Experiment

The measurement of the $^{14}\text{N}(d, p)$ reaction used the FSU tandem-linac accelerator system to produce the 16 MeV deuteron beam that bombarded a melamine ($\text{C}_3\text{H}_6\text{N}_6$) target. A silicon surface barrier ΔE – E telescope was used to collect the d elastic and p transfer data at laboratory angles of 10–35° in steps of 5°. A fixed monitor detector was used to determine the relative angular distribution for the elastic and proton transfer data and to provide a continuous monitor of the target thickness since melamine has a low melting point and it is possible that target material could boil away during the experiment. The beam current was kept below 15 pA and no target changes were observed during the experiment. The elastic scattering data in the movable detector were matched to previously measured elastic deuteron–carbon and nitrogen [13] scattering to get the absolute cross section values. Based on the absolute cross section of the published d – ^{12}C , ^{14}N scattering data and the statistics gathered in the present run, the absolute cross section is accurate to $\pm 20\%$. Since the emphasis in the current work was on the investigation of the single neutron strength of high lying states in ^{15}N , the detector gains were set so that no data were taken for the ground state transition. Previously published data exist [2] and these were

used in the current analysis. As can be seen in the typical spectrum shown in Fig. 1, the carbon and hydrogen in the target provide significant overlaps with the states of interest. To make certain that no peak coming from a contaminant was misidentified as one in ^{15}N , a scattering chamber was filled with pure nitrogen gas and spectra were obtained at the same angles as with the melamine target. While these spectra have worse energy resolution due to the beam and ejectile straggling and energy loss of the particle in the gas, they showed that no states populated in ^{15}N were missed or covered up by the presence of the hydrogen and carbon in the melamine target.

3. Results

The measured angular distributions of the ^{15}N states were compared to calculated Finite-range Distorted Wave Born Approximation (DWBA) angular distributions, performed using the code *Fresco* [14], to extract the relative single particle spectroscopic strengths. Deuteron and proton optical model potentials were taken from Phillips and Jacobs [3]. The deuteron bound state wave function was calculated using the Reid soft core potential [16] and the transferred neutron was bound to the ^{14}N core in a well of Woods–Saxon shape of radius $1.25 \times A^{1/3}$ fm and diffuseness 0.65 fm with a spin–orbit component of the usual Thomas form and depth of 6 MeV, and the same radius and diffuseness parameters as the central part; the depth of the central part was adjusted to give the correct binding energy. The calculations were performed using the post form of the DWBA and included the full complex remnant term.

Figure 2 shows the angular distributions that we have identified as being described as primarily arising from an $L = 0$ transfer, and Fig. 4 are those arising from a dominant $L = 2$ transfer. Also, shown in Fig. 3 is the $L = 1$ transfer to the 6.323 MeV state. The spectroscopic factors for the transfers were determined by normalizing the DWBA calculations to the experimental data. Table I compares the neutron spectroscopic factors extracted from the current work with those from the previous work of Phillips and Jacobs [3] as well as the results of the shell model calculations.

As can be seen, there is good agreement between the values extracted by Phillips and Jacobs [3] in their 9 MeV study and the present work so that the normal concern of the possible dependence on bombarding energy due to non-direct neutron transfer is not a factor in describing the strong transitions. However, a major difference observed in the $^{14}\text{N}(d, p)$ spectrum in Fig. 1 is the population of states around 9 MeV in excitation, which are much more strongly populated at the low bombarding energy of 3 MeV [15] than in the present work showing that for these states, compound processes are very important at the lower energy so that these low energy data cannot be used to extract meaningful spectroscopic factors.

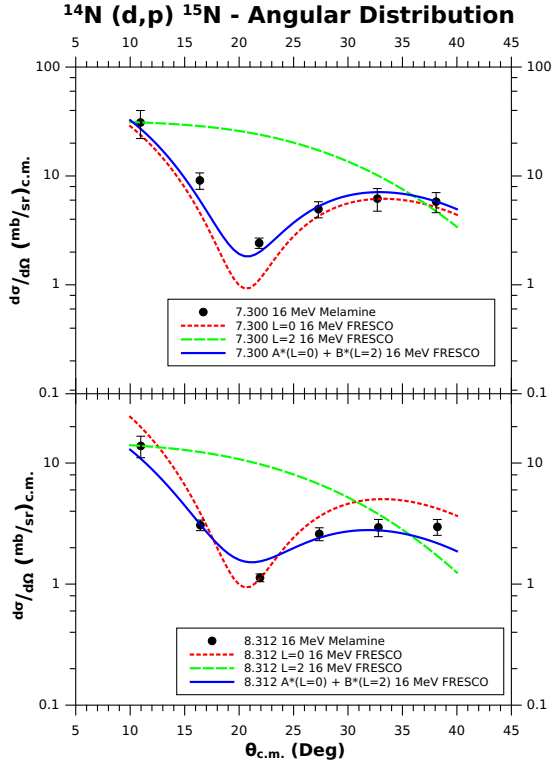


Fig. 2. Angular distributions of $L = 0$ transfer dominant states identified in the $^{14}\text{N}(d, p)$ reaction.

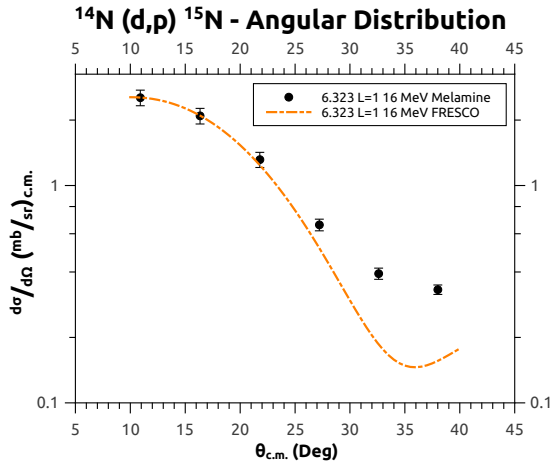


Fig. 3. Angular distribution of $L = 1$ dominant state identified in the $^{14}\text{N}(d, p)$ reaction.

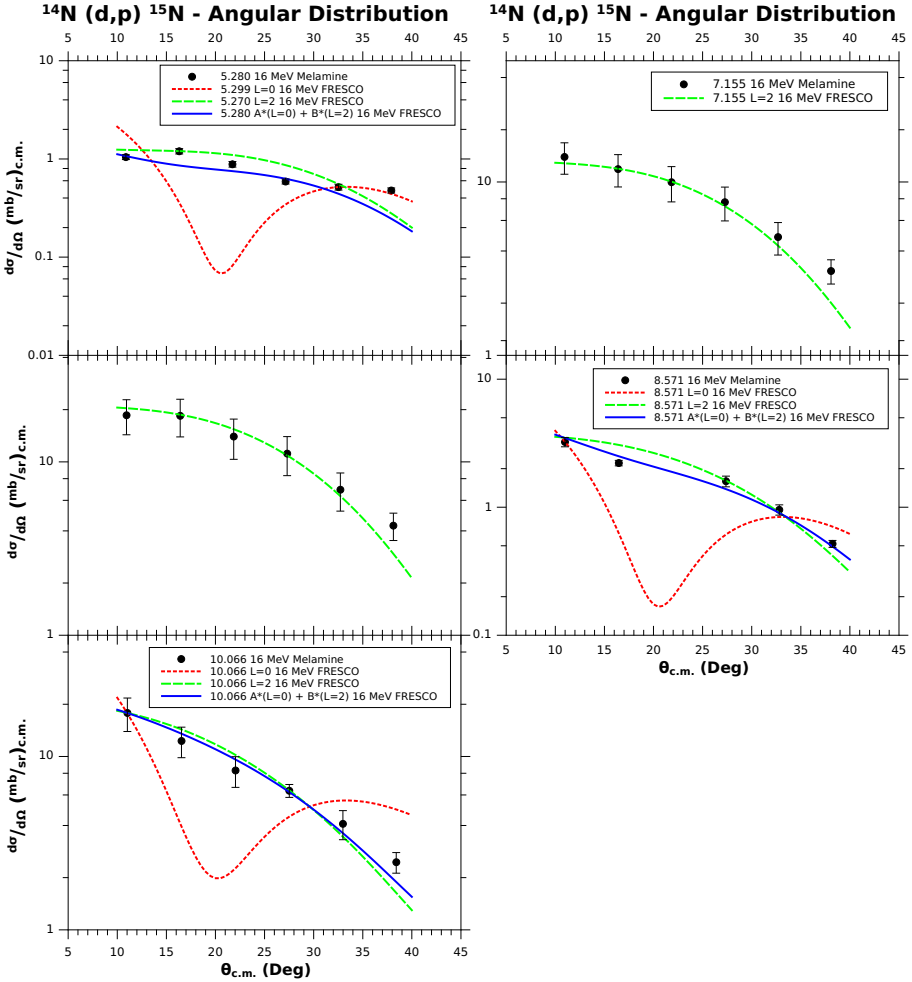


Fig. 4. Angular distributions of $L = 2$ dominant states identified in the $^{14}\text{N}(d, p)$ reaction.

The total $2s_{1/2}$ and $1d_{5/2}$ neutron strength is spread over numerous states because the ground state of ^{14}N has a spin and parity of 1^+ . This means that the neutron strength of the $2s_{1/2}$ level will be found in final states of spin parity $1/2^+$ and $3/2^+$, while that of the $1d_{5/2}$ level will be found in $3/2^+$, $5/2^+$, and $7/2^+$. For the $3/2^+$ states which can be populated by both $L = 0$ and $L = 2$ transfer, a best fit to the angular distribution was formed. The summed spectroscopic strengths were found by forming the sums of the respective single particle strengths. Then, the energy weighted summed strengths, which can be found in Table II, were calculated to determine the splitting between the $s_{1/2}$ and $d_{5/2}$ neutron orbits for the three sets of data.

TABLE I

 Spectroscopic factors for the $^{14}\text{N}(d, p)^{15}\text{N}$ reaction.

| ^{15}N State | J^π | Nucleus state | L value | 16 MeV | Theoretical | 9 MeV* |
|-----------------------|---------|---------------|-----------|------------------|-------------|-----------------|
| 5.280** | $1/2^+$ | $s_{1/2}$ | $L = 0$ | 0.02 ± 0.004 | 0.39 | < 0.05 |
| | $5/2^+$ | $d_{5/2}$ | $L = 2$ | 0.10 ± 0.020 | 0.11 | < 0.05 |
| 6.323 | $3/2^-$ | $p_{3/2}$ | $L = 1$ | 0.20 ± 0.040 | 0.02 | 0.10 ± 0.02 |
| 7.155 | $5/2^+$ | $d_{5/2}$ | $L = 2$ | 0.98 ± 0.020 | 0.65 | 0.88 ± 0.03 |
| 7.300 | $3/2^+$ | $s_{1/2}$ | $L = 0$ | 1.10 ± 0.024 | 0.72 | 0.89 ± 0.04 |
| | | $d_{5/2}$ | $L = 2$ | 0.11 ± 0.008 | 0.07 | 0.07 ± 0.05 |
| 7.567 | $7/2^+$ | $d_{5/2}$ | $L = 2$ | 1.05 ± 0.020 | 0.73 | 0.87 ± 0.01 |
| 8.312 | $1/2^+$ | $s_{1/2}$ | $L = 0$ | 0.89 ± 0.004 | 0.65 | 1.02 ± 0.04 |
| | | $d_{3/2}$ | $L = 2$ | 0.27 ± 0.030 | 1.74E-004 | < 0.09 |
| 8.571 | $3/2^+$ | $s_{1/2}$ | $L = 0$ | 0.04 ± 0.020 | 5.21E-006 | 0.02 ± 0.01 |
| | | $d_{5/2}$ | $L = 2$ | 0.21 ± 0.026 | 0.13 | 0.12 ± 0.03 |
| 10.066 | $3/2^+$ | $s_{1/2}$ | $L = 0$ | 0.15 ± 0.013 | 0.04 | 0.32 ± 0.08 |
| | | $d_{5/2}$ | $L = 2$ | 0.86 ± 0.008 | 0.55 | 0.48 ± 0.08 |

* — Data extracted from [3].

 ** — The energy resolution was not sufficient to separate the 5.270 and 5.299 MeV states of ^{15}N .

TABLE II

 Sum rule and centroid locations for $s_{1/2}$ and $d_{5/2}$ neutrons in ^{15}N .

| | 16 MeV | Theoretical | 9 MeV |
|------------------------------------|-----------|-------------|------------|
| Sum Rule ($s_{1/2} \otimes 1^+$) | | | |
| $J^\pi = 1/2^+$ | 0.910 | 0.760 | 1.230 |
| $J^\pi = 3/2^+$ | 1.254 | 0.656 | 1.040 |
| Sum Rule ($d_{5/2} \otimes 1^+$) | | | |
| $J^\pi = 3/2^+$ | 1.174 | 0.823 | 0.600 |
| $J^\pi = 5/2^+$ | 1.080 | 0.763 | 0.930 |
| $J^\pi = 7/2^+$ | 1.050 | 0.731 | 0.870 |
| Centroid ($s_{1/2}$) | 7.904 MeV | 7.835 MeV | 8.138 MeV |
| Centroid ($d_{5/2}$) | 8.068 MeV | 8.016 MeV | 7.918 MeV |
| $\Delta (d_{5/2} - s_{1/2})$ | 0.164 MeV | 0.181 MeV | -0.220 MeV |

As Table II shows, the location of the centroids for each of the sets of data is roughly the same, and therefore independent of the bombarding energy producing ^{15}N . The summed strength over each neutron state is of the order of unity. This, in conjunction with the theoretical calculations, shows that all the major $2s_{1/2}$ and $1d_{5/2}$ single neutron particle strengths in $^{14}\text{N}(d, p)$ were found.

4. Conclusion

The present work shows that the extracted spectroscopic strengths at the higher deuteron bombarding energy used here agree well with those previously extracted from the $^{14}\text{N}(d, p)$ reaction at what was considered a low enough energy (9 MeV) that compound nucleus contributions might be important. However, the current agreement shows that the assumption by Phillips and Jacobs that the (d, p) reaction was direct at their lower energies is correct. The neutron energy centroids extracted here show that the neutron $s_{1/2}$ and $d_{5/2}$ orbits are roughly degenerate. This means that the energy splitting of these two orbits changes rapidly around ^{15}N since in ^{13}C the $s_{1/2}$ orbit is 760 keV below the $d_{5/2}$ orbit, while in ^{17}O , the $s_{1/2}$ orbit is 870 keV above the $d_{5/2}$ orbit. This work also demonstrates that modern p - sd shell model calculations reliably reproduce this trend as well as being able to predict total neutron orbit strengths in light nuclei.

REFERENCES

- [1] D. Kurath, *Phys. Rev.* **101**, 216 (1956); E.C. Halbert, J.B. French, *Phys. Rev.* **105**, 1563 (1957); A.M. Lane, *Rev. Mod. Phys.* **32**, 519 (1960).
- [2] J.P. Schiffer *et al.*, *Phys. Rev.* **164**, 1274 (1967).
- [3] G.W. Phillips, W.W. Jacobs, *Phys. Rev.* **184**, 1052 (1969).
- [4] S. Lie, T. Engeland, *Nucl. Phys.* **A267**, 123 (1976) and references in there.
- [5] F. Ajzenberg-Selove, *Nucl. Phys.* **A152**, 1 (1970).
- [6] H.G. Bingham, H.T. Fortune, J.D. Garrett, R. Middleton, *Phys. Rev. Lett.* **26**, 1448 (1971).
- [7] C.H. Holbrow, H.G. Bingham, R. Middleton, J.D. Garrett, *Phys. Rev.* **C9**, 902 (1974).
- [8] N. Anyas-Weiss *et al.*, *Phys. Rep.* **12**, 201 (1974); H.G. Bingham *et al.*, *Phys. Rev.* **C11**, 1913 (1975).
- [9] C. Lee *et al.*, *Phys. Rev.* **C60**, 024317 (1999).
- [10] Y. Utsuno, S. Chiba, *Phys. Rev.* **C83**, 021301(R) (2001).
- [11] A. Volya, Y.M. Tchuvil'sky, to be presented IASSEN 2013, <http://iasen-2013.jinr.ru>
- [12] A. Volya, *Phys. Rev.* **C79**, 044308 (2009); <http://cosmo.volya.net>
- [13] N. Jarmie, J.H. Jett, R.J. Semper, *Phys. Rev.* **C10**, 1748 (1974).
- [14] I.J. Thompson, *Comput. Phys. Rep.* **7**, 167 (1988).
- [15] A. Amokrane *et al.*, *Phys. Rev.* **C6**, 1934 (1988).
- [16] R.V. Reid Jr., *Ann. Phys. (NY)* **50**, 441 (1968).